Microbiology, Metabolites and Biotechnology
Journal home page: https://mmb.irost.ir
MMB
The former ARMMT

Theoretical and Experimental Study of a Glycan-Coated Biosensor for *Staphylococcus aureus* Detection

Vahidreza Nafisi[1]*, Ensieh Fahimi Kashani[2], Zahra Mousavian[3], Yasamin Bide[4], Alireza Balaei[1]

[1] *Department of Electrical Engineering and Information Technology, Iranian Research Organization for Science and Technology (IROST), Tehran, Iran.*
[2]*Department of Stem Cells and Developmental Biology, Cell Science Research Center, Royan Institute for Stem Cell Biology and Technology, ACECR, Tehran, Iran.*
[3]*Department of Biotechnology, Iranian Research Organization for Science and Technology (IROST), Tehran, Iran.*
[4] *Department of Chemical Technologies, Iranian Research Organization for Science and Technology (IROST), Tehran, Iran.*

Article Info

Document Type:
Research Paper

Received 24/09/2025
Received in revised form 20/11/2025
Accepted 08/12/2025

Keywords:
Molecular docking simulation,
Biosensors,
GA2 ganglioside

Abstract

Methicillin-resistant *Staphylococcus aureus* is one of the community-associated pathogens with a high capacity for attachment to human tissues and biofilm formation. Therefore, the design of tools for rapid identification of this bacterium in environments and providing timely safety alerts is essential for public health. The aim of the present study was to identify a suitable coating that can be immobilized on an electrical sensor and effectively capture *Staphylococcus* cells on the sensor surface. The glycan Asialoganglioside GM2 (GA2) was selected as a candidate for this purpose, and molecular docking simulations were used to investigate and validate its potential to bind Staphylococcus receptors. The results showed that the interaction of GA2 with *S. aureus* receptors exhibited high binding affinity and relatively low RMSD values, indicating a stable and reliable binding interaction. This strong binding of GA2 with ClfB receptor suggests potential applications for GA2 in inhibiting bacterial adhesion and in developing diagnostic or therapeutic strategies targeting *S. aureus*. Also, this simulation finding was confirmed experimentally. A GA2 coating was applied to the sensor, increasing the probability of bacterial attachment to the sensor surface by more than eightfold. Also, the coating's specificity to *S. aureus* detection was examined with *E. coli* (experimentally and theoretically). These findings may provide a basis for designing targeted therapeutics and diagnostics against this important pathogen.

1. Introduction

Infections caused by *Staphylococcus aureus* are a serious threat to public health worldwide. Methicillin-resistant strains of this bacterium (MRSA) have a high ability to adhere to human tissues, form biofilms, and evade the host immune response, and are known to be one of the most common causes of hospital-acquired infections, respiratory tract infections, surgical wound infections, and sepsis (Foster *et al.,* 2014; Tong *et al.,* 2015). Airborne MRSA may also cause respiratory disease, so rapid detection and the design of real-time diagnostic tools are required (Zelada-Guillén *et al.,* 2012). Given the clinical importance of this pathogen, identifying ligands that specifically and strongly bind to *S. aureus* surface receptors can play an important role in designing new diagnostic and therapeutic methods. These ligands are particularly useful for detecting early-stage infections, where a prompt clinical response can make a critical difference (Eswar *et al.* 2006; Varki 2007).

S. aureus delivers a set of reagents of cell-wall-bound proteins, which facilitates the connection to the host's extracellular matrix constituents, fibrinogen, and platelets. ClfB, FnBPA, SasG, and collagen-binding domains are the most significant surface receptors for host attachment and early pathogenesis. One of the most important surface receptors of *S. aureus* is the Clumping factor B (ClfB) protein, which binds to the C-terminal domain of keratin-10 (one of the major constituents of the squamous epithelial cells). The process helps successfully colonize the upper respiratory tract, and the bacteria are then aspirated into the lungs, contributing to infections like pneumonia (Walsh *et al.,* 2008).

ClfB has certain characteristics that make it an appealing target for the design of specific ligands to detect real-time *S. aureus*. FnBPA is a fibrinogen and fibronectin binding protein that is involved in initial adherence to host surfaces, internalization into endothelial cells, and stimulation of inflammation.

SasG includes serine-aspartate repeats and G5-E domains that enhance bacterial aggregation and dense biofilm formation, thereby supporting the long-term persistence of *S. aureus* in protein-rich humid conditions such as airways and alveoli. SasG also interacts with other

*Corresponding author E-mail: vr_nafisi@irost.org
DOI: 10.22104/mmb.2025.7874.1184

adhesins to enhance immune evasion and the persistence of chronic infections. Accordingly, it has been suggested that ClfB, FnBPA, and SasG are optimal targets to be used in designing specific ligands that can be used to detect *S. aureus* rapidly and sensitively (Berry *et al.,* 2022; Foster *et al.,* 2014; Ganesh *et al.,* 2008; Ghali *et al.,* 2016; Crosby *et al.,* 2017; Otto 2013; Reddinger *et al.,* 2016; Schwermann & Winstel, 2023; Wertheim *et al.,* 2008). The design of targeted therapeutics and the subsequent diagnostic and treatment courses against this significant pathogen could also be encouraged by such approaches (Brooks *et al.,* 2009; Forli *et al.,* 2016).

Among the traditional and rational drug design methods, the structure-based drug design is considered more efficient and cost-effective. This method is also based on the concept of reverse pharmacology, which involves first identifying a specific protein of interest and then selecting a small-molecule candidate from a library based on its affinity for the protein of interest (Singh & Bhattacharjee, 2024).

The structure-based drug design implemented in this study used molecular docking and molecular dynamics, the most common and reliable approaches available in this field. Such computational methods allow for in-depth study of ligand-protein interactions, structural dynamics, binding energies, and other related phenomena.

In this study, the glycan Asialoganglioside GM2 (GA2) was chosen as a ligand because it is specifically recognized by surface adhesins of *S. aureus* and plays an important role in bacterial adhesion and colonization. Initial docking results suggested that GA2 shows a strong affinity for the active site of ClfB in *S. aureus*.

To assess the specificity of GA2, the CFA/I pili receptor of *Escherichia coli* was selected as a negative control, representing a Gram-negative bacterium and a common causative agent of gastrointestinal infections. The CFA/I pili receptor has a well-characterized crystalline structure and plays a key role in gut colonization (Croxen *et al.,* 2013; Martínez-Alonso *et al.,* 2008; Nataro & Kaper, 1998; Zhang *et al.,* 2022).

This comparison allowed evaluation of GA2 interactions with two major bacterial groups, Gram-positive (*S. aureus*) and Gram-negative (*E. coli*), and facilitated a more accurate assessment of GA2 specificity for *S. aureus*.

Overall, an integrated approach was used to gain a deeper understanding of the molecular dynamics of interactions between GA2 and its bacterial receptors. After assessing the *in-silico* binding potential, an experimental testbed was designed and constructed to evaluate the practical capture efficiency of GA2 on *Staphylococcus* cells.

2. Materials and Methods

The study proceeded in two main phases. First, the binding potential of three surface receptors from *Staphylococcus* and one adhesin from *E. coli* to the GA2 glycan was evaluated using molecular docking simulations (Section 2.1). Then, after confirming strong and stable in-silico interactions between GA2 and *S. aureus* receptors, an in vitro experiment was designed (Section 2.2).

2.1. Simulation

2.1.1. Software and computational resources

The molecular docking simulation process was performed using various bioinformatics tools, including AutoDock Vina (for docking and binding affinity scoring), AutoDock Tools (for ligand and receptor preparation and grid box setup), PyMol (for 3D structural visualization and pre-processing), GROMACS (for molecular dynamics simulation and energy minimization), as well as online databases and servers such as SWISS-MODEL (for homology modeling), RCSB PDB (for obtaining crystal structures of target proteins), NCBI (for retrieving gene and protein information), DrugBank (for collecting drug-related biochemical data), and ChemSpider (for chemical structure retrieval). Visualization and analysis of docking results were carried out using BIOVIA Discovery Studio Visualizer (for interaction analysis and 2D/3D binding visualization).

2.1.2. Receptor and ligand preparation

Protein preparation in Discovery Studio involved the removal of chloride and calcium ions, water molecules, and non-essential ligands. In PyMOL, each receptor residue was protonated as required. The active site and protein functional groups were preserved.

Active site locations for the bacterial receptors were identified using AutoDock Tools, based on the literature (Ganesh *et al.,* 2011; Li *et al.,* 2007). Final receptor files were saved in pdbqt format to retain essential (polar) hydrogens for docking.

Ligand structures were generated using online servers such as SWISS-MODEL and optimized in MOE for stereochemical accuracy. All structures were energy-minimized using GROMACS to remove atomic clashes and optimize conformational energies.

2.1.3. Docking procedure

Crystal structures of the *S. aureus* ClfB receptor (subspecies N315, PDB ID: 3ASW) and the *E. coli* CFA/I pili (PDB ID: 3F83) were obtained from the Protein Data Bank. The three-dimensional structure of the ligand Asialoganglioside GM2 (GA2) was downloaded from PubChem in SDF format.

ClfB and CFA/I pili modeled structures were examined in silico. First, the important residues found at the active sites include Lys107, Asn197, and Gln358 in CFA/I pili (Figure 1-A), as well as Val528, Glu525, Asn234, and Ser236 in ClfB (Figure 1-B) (Ganesh *et al.,* 2011; Li *et al.,* 2007).

Second, blind docking analyses were performed, allowing GA2 to explore the entire protein surface, and the resulting low-energy clusters consistently localized within the same pockets identified in the literature.

These residues' interactions with the GA2 glycan were then predicted using AutoDock Vina and Discovery Studio, and the docking poses were ranked based on binding energy, clustering behavior (RMSD), and the presence of key hydrogen-bonding and hydrophobic interactions.

Prepared receptor and ligand files were loaded into AutoDock Tools, and a grid box was defined to encompass all key residues within the binding pocket. The grid dimensions and spacing were refined based on initial structural inspections and binding-site assessments performed in Discovery Studio (preliminary analyses), which helped determine the appropriate boundaries to ensure complete coverage of the interaction region. Docking was performed in a ligand-flexible/receptor-rigid mode, allowing the ligand to explore multiple conformations while keeping the receptor fixed. To ensure adequate conformational sampling, 100 independent docking runs were carried out. Output poses were ranked by AutoDock Vina binding energy scores, and complexes with the lowest predicted free binding energies were selected for further analysis. Non-covalent interactions (hydrogen bonds, van der Waals interactions, and hydrophobic contacts) were characterized on these poses. Three-dimensional visualization and interaction mapping were produced in BIOVIA Discovery Studio Visualizer and PyMOL to localize contact residues and interaction patterns.

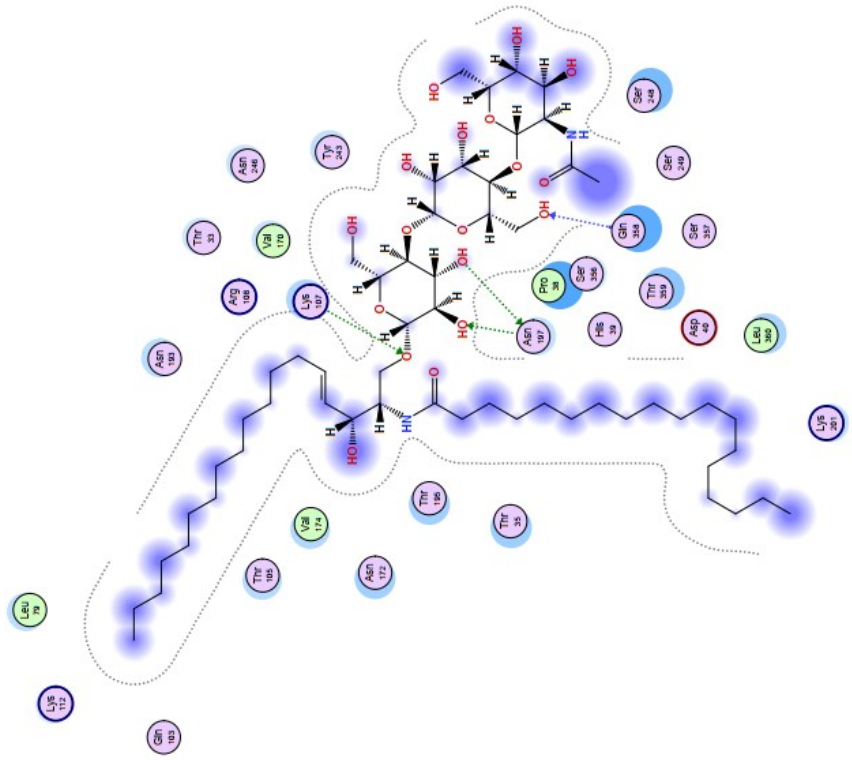

(A)

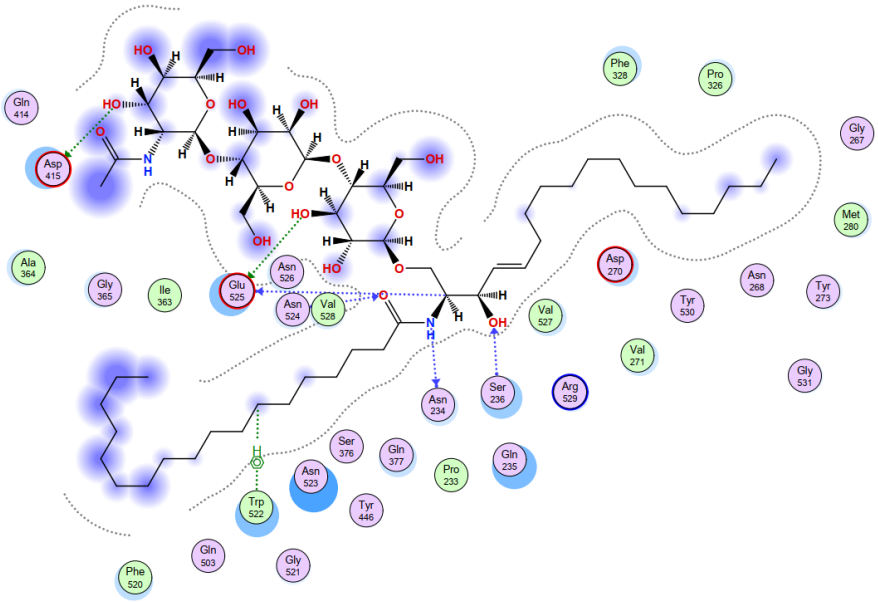

(B)

Figure 1. The best residues for interaction of (A) CFA/I pili of E.coli and (B) ClfB of *S. aureus* with ASIALOGANGLIOSIDE-GM2 glycan.

2.1.4. Complex stability assessment

To quantify the strength and stability of receptor-ligand interactions, molecular dynamics (MD) simulations were executed using GROMACS 5.1.1 with the GROMOS96 43a1 force field. Complexes were solvated in a cubic water box with periodic boundary conditions to create a fully hydrated simulation environment. The system was then neutralized by adding appropriate counterions. Energy minimization was subsequently performed using the steepest-descent algorithm to eliminate steric clashes and resolve any unfavorable atomic contacts before initiating the dynamics.

Following energy minimization, the solvated systems were prepared using a cubic SPC/E water box, and charge neutrality was achieved by adding Na^+ or Cl^- counterions via the GROMACS genion module. Temperature coupling during equilibration was performed using the V-rescale thermostat at 300 K, while pressure coupling in the NPT phase was carried out using the Parrinello–Rahman barostat at 1 bar. The number of solvent molecules and ions was automatically determined based on the dimensions of the simulation box generated for each ligand–receptor complex.

Equilibration stages were performed in NVT and NPT ensembles to stabilize temperature and pressure, respectively. Production MD runs were carried out for 50 ns at 300 K with coordinates recorded every 2 ps. Dynamics of the complexes were monitored to assess stability. Structural metrics such as RMSD and RMSF were calculated using GROMACS tools to quantify the strength and stability of receptor ligand interactions. Binding energy calculations were performed to quantify interaction strength and stability.

2.2. Experimental test setup

With a forward-looking objective aimed at airborne pathogen detection, a controlled environment for the release of airborne particles, their entry into the sampling unit, and their deposition on the surface of a biosensor was designed. This test setup consists of the following components (Figure 2-A):

- 2-liter spherical chamber with connections to the nebulizer chamber, sampling units, flow pump, and reference Falcon tube.
- Nebulizer: A Philips Respironics nebulizer was used to create the necessary pressure required to nebulize the solution in the tank. This nebulizer converts the produced suspension into bioaerosol particles of various sizes in the micron range. The nebulizer flow rate is approximately 2 liters per minute. Three milliliters of each desired bacterial solution were placed in the nebulizer's plastic tank (with a capacity of 10 milliliters).
- A Falcon tube containing 15 to 17 milliliters of liquid culture medium was used as a reference to confirm the presence of bacteria in the test setup.
- Two cascade-impactor samplers composed of four separation stages (A-D) that fractionate particles from the air stream according to particle aerodynamic diameter (Figure 2-B). The two samplers were run in parallel for comparison.
- Suction pumps draw ambient air into the samplers, along with particles. The system flow can be adjusted up to approximately 11 L/min.
- The environmental conditions were: ambient temperature of 25 ºC ± 2 ºC and humidity of 35% ± 5%.

To evaluate the effect and capture efficiency of the GA2 bio-coating, it was necessary to ensure that it was stably immobilized on the sensor surface. The chemical substances used to treat the sensor surface are shown in Table 1. The ganglioside (GA2) was dissolved in Methanol:Chloroform (2:1), stored at -20 °C, and then dispersed in TBS (Tris-buffered saline). To achieve a uniform and high-quality final coating, a spin-coating method was used. In this approach, the droplet was placed on the sensor surface, which was then rotated at a specified speed within a chamber to spread the droplet uniformly across the sensor (Figure 3).

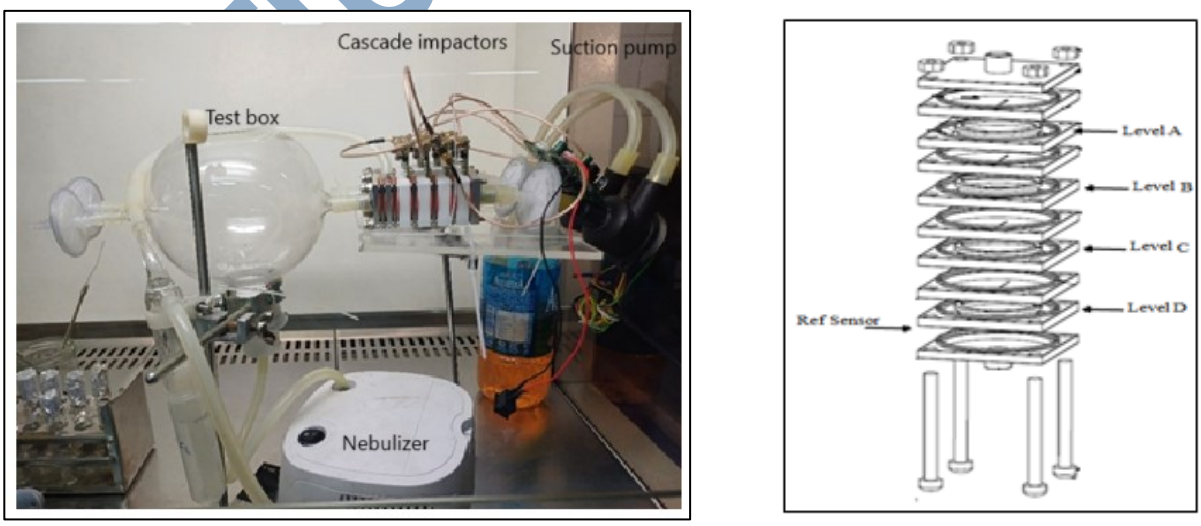

(A) (B)

Figure 2. (A) Experimental test setup for microbial test (B) Four-stage cascade impactor structure

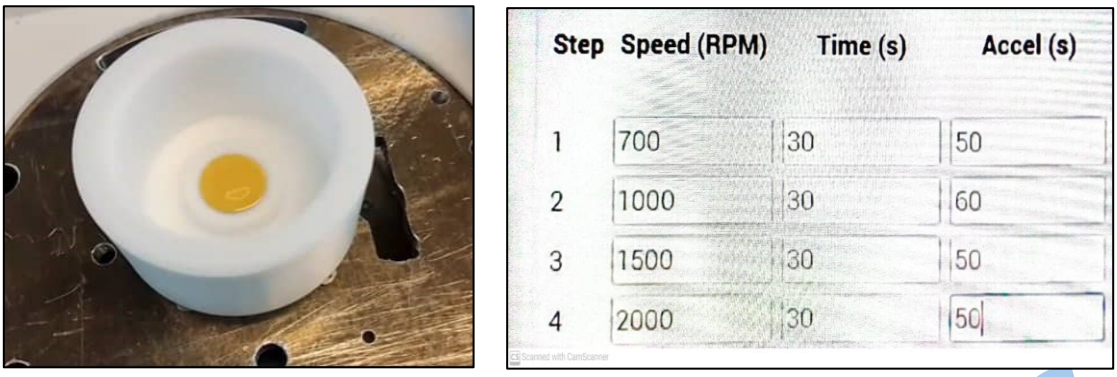

Figure 3. Spin-coating device (hardware and software) for the last stage of the coating procedure: Spin-coating chamber with the sensor in place (left); Spin-coating speed, acceleration, and time settings (right).

Table 1. The materials used for the coating stages

Material	Merck Code	Cas. No.
11-mercapto-undecanoic acid (MUA)	450561	71310-21-9
4-morpholine ethane sulfonic acid sodium salt (MES) buffer	M3885	71119-23-8
Sodium Chloride: NaCl	S9888	7647-14-5
1-ethyl-3-(-3-dimethylaminopropyl) carbodiimide hydrochloride (EDC)	E6383	25952-53-8
N-hydroxysuccinimide (NHS)	130672	6066-82-6
Phosphate buffer saline (PBS) pH=7.4		

To evaluate the amount of bacteria trapped on the sensor surface, at the end of the test, the sensors were placed in plates containing normal saline and Triton buffer, a buffer used to detach bacteria from the surface. The plates were placed on a shaker at 200 rpm for 30 minutes. Then, 100 microliters from each well of the six-well plate assigned to a sensor were cultured on nutrient agar plates. Additionally, 100 microliters from the liquid in the Falcon tube were also taken and cultured on agar plates. The colony count from the culture of the Falcon tube liquid was used as a reference. Finally, the nutrient agar plates were incubated at 37°C for 24 hours, and after the incubation period, the number of bacterial colonies was counted.

To evaluate the quality of the coating method, ATR-FTIR (Tarbiat Modares University, Iran) and FESEM (Central Laboratory, IROST, Iran) analyses were performed.

3. Results and Discussion

3.1. Primary metrics evaluation

Initially, key metrics, including binding energy and root-mean-square deviation (RMSD), for the ligand complexed with the target receptors were examined (Table 1). In this analysis, *E. coli* (PDB: 3F83) was used as a Gram-negative reference alongside *S. aureus* receptors as Gram-positive targets.

The evaluation showed that both GA2-ClfB and GA2-CFA/I complexes had RMSD values below 2 Å, indicating valid and stable ligand placement in the binding pocket (Leach *et al.,* 2006). The RMSD value in the ClfB complex was slightly higher than in the CFA/I complex (1.8750 versus 1.4974 Å). However, the binding energy of GA2 to ClfB was found to be significantly stronger than that of CFA/I (-12.10 versus -10.60 kcal/mol). This discrepancy implies that the GA2 ligand establishes numerous hydrogen and hydrophobic contacts with the receptor, resulting in superior stereochemical compatibility than CFA/I. In addition to the binding energy and RMSD values, a hydrogen-bond analysis was performed to further characterize ligand–receptor specificity. The GA2–ClfB complex exhibited seven conventional hydrogen bonds and three carbon-hydrogen bonds, totaling approximately ten hydrogen-bond interactions. In contrast, the GA2–CFA/I complex formed five conventional and two carbon-hydrogen bonds (≈7 total interactions). The denser hydrogen-bond network in the GA2–ClfB complex is consistent with its stronger binding affinity and suggests a structurally more favorable interaction pattern for *S. aureus* recognition. In addition to hydrogen bonding, the GA2–ClfB complex exhibited a dense network of van der Waals interactions (ILE363, ALA364, GLY365, SER376, GLN377, GLY521, TRP522, PHE520, VAL527, VAL528, PHE328, MET280, TYR273, PRO326, etc.) as well as several hydrophobic/alkyl contacts (VAL528, PHE328, MET280, TYR273, PRO326). In contrast, the GA2–CFA/I complex showed only sparse hydrophobic contacts (VAL170, LEU360) and weaker, more dispersed van der Waals interactions. This difference in non-polar interactions further supports the stronger binding affinity of GA2 toward ClfB. Consequently, the GA2-CFA/I interaction reveals reduced binding energy and a less stable complex due to inadequate complementarity of the hydrophobic and polar areas of the receptor.

In contrast, the GA2-ClfB complex with a higher binding energy and a more stable interaction pattern confirms the specificity of GA2 for the ClfB receptor and highlights its high potential for identifying *Staphylococcus aureus* in future pharmacological and biological studies.

To summarize, GA2 demonstrated stronger binding affinity toward the S. aureus ClfB receptor compared with the CFA/I adhesin of E. coli. Specifically, GA2 formed a denser hydrogen-bonding network and more favorable

hydrophobic contacts with ClfB, as reflected in its lower binding energy (−12.10 kcal/mol vs. −10.60 kcal/mol) and more stable RMSD values. Table 2 summarizes these key quantitative differences.

Table 2. Molecular docking results of Asialoganglioside GM2 (GA2) with surface receptors of *S. aureus* and *E. coli.*

Compound	Rseq	Δ binding energy (kcal/mol)	RMSD (Å)
3ASW_GA2	1	-12.1042	1.8750
3F83_GA2	1	-10.6086	1.4974

3.2. *In-silico* evaluation of GA2

GA2 was identified as a key ligand for *S. aureus* with a binding energy of -12.1042 kcal/mol (RMSD: 1.8750 Å) for ClfB and -10.6086 kcal/mol (RMSD: 1.4974 Å) for *E. coli*. This indicates a higher binding affinity with *S. aureus* receptors. Molecular dynamics simulations provided a realistic depiction of complex behavior in a simulated biological environment and, in addition to confirming complex stability, yielded valuable information for further analyses and potential ligand optimization.

Molecular docking results provide valuable insights into ligand–receptor interactions for *S. aureus* and *E. coli*. The binding energies and RMSD values indicate the level of binding propensity and structural complementarity, which is essential for determining ligands that are therapeutically and pharmacologically useful.

GA2 also exhibited extremely robust affinity to the ClfB receptor of *S. aureus* (3ASW) with an affinity energy of -12.1042 kcal/mol (RMSD: 1.8750 A) but showed weaker affinity to the E. coli receptor (3F83) with an affinity energy of -10.6086 kcal/mol (RMSD: 1.4974 A). The binding energy is very high, but the RMSD is relatively low, which should be attributed to the presence of a large number of hydrogen bonds and optimized hydrophobic areas in the binding pocket, resulting in the considerable stability of the GA2-ClfB complex.

The results indicate that GA2 may selectively attach to ClfB and be effective in inhibiting the ability of *S. aureus* to adhere to host tissues, which is appropriate given the key role of ClfB in pathogenesis (Foster *et al.,* 2014).

Singh & Bhattacharjee (2024) examined the adhesin proteins ClfA and ClfB to develop a ligand molecule that inhibits their binding to the host surface.

By comparing various metrics, they discovered that the binding energies of the identified compounds with ClfA and ClfB (-10.37 and -11.11 kcal/mol, respectively) were greater than those of allantodapsone with ClfA and ClfB. They additionally developed allantodapsone, a ClfA and C1fB inhibitor that has been demonstrated to have anti-colonizing abilities *in vitro* (Singh & Bhattacharjee, 2024).

These binding sites were detailed and mapped, and the specific amino acid residues in each receptor were shown to be the determinants of specificity and stability of interaction.

Such residues as Val528, Glu525, Asn234, and Ser236 were recognized as hot spots that are incorporated into a network of hydrogen bonds and hydrophobic interactions in the GA2/ClfB complex to provide stable accommodation of the ligand. In the GA2CFA/I-complex (*E. coli*), on the other hand, the residues, which included Lys107, Asn197, and Gln358, were only involved in more restrictive interactions, which were more hydrophobic or weakly electrostatic in nature and had less binding energy. This variation in the pattern of interactions highlights the stereochemical and chemical complementarity between the ClfB binding pocket and the GA2 structure and explains GA2's preference for binding *S. aureus* over *E. coli* (Ganesh *et al.,* 2008; Leach *et al.,* 2006; Li *et al.,* 2007).

In general, the findings suggest that the ClfB receptor of *S. aureus* has maximized the interaction properties of GA2. The binding and structural complementarity between GA2 and ClfB indicate that GA2 could be used to prevent bacterial adhesion and to develop diagnostic or therapeutic options against *S. aureus*.

3.3. *In-vitro* evaluation of GA2

To validate the *in-silico* results, a series of *in vitro* experiments was conducted using the cascade impactor described in Section 2.2. Initially, GA2 should be immobilized on the sensor surface through specific chemical treatments using the materials listed in Table 1. The quality of each coating step was assessed by FTIR spectroscopy.

Figure 4-A illustrates the surface morphology of the untreated sensor. Following ozone treatment combined with ultraviolet irradiation (181 nm wavelength) for 30–45 minutes, a significant reduction in surface impurities was observed, as shown in Figure 4-B.

After this step and ultrasonic polishing with alumina, the QCM crystal is cleaned by exposing it to a piranha solution (1 part hydrogen peroxide by volume to 3 parts sulfuric acid by volume).

After 5 min, the crystals are removed and rinsed twice with DI water and then twice with ethanol Then the sample is dried under a nitrogen stream for 5 min. The sensor from the previous step is incubated in a 5 mM MUA ethanol solution at pH 2.0 for 48 hours. After washing with ethanol and DI water, it is immersed in a 0.1 M MES buffer containing 0.5 M NaCl at pH 5.8. Next, EDC and NHS are added to the buffer to reach final concentrations of 2 mM and 5 mM, respectively. After 40 min, the solution is removed, and the sensor is washed with DI water and MES buffer respectively. Finally, this chemically treated sensor surface was exposed to 100 µL of GA2 solution via the spin coating method. The sensor was kept overnight in an appropriate storage environment.

The ATR-FTIR analysis of the final coating is shown in Figure 5. The peaks around 2900-3000 cm^{-1} (acidic OH group) and 1700 cm^{-1} (carbonyl group) were observed in the spectrum after the coating steps.

The morphology of the sensor surface treated with MUA-EDC/NHS and the GA2-coated sensor, as assessed by FESEM, is shown in Figure 6 (left and right, respectively) at three different magnifications (2.00k×, 10.00k×, and 35.00k×). The FESEM images suggest that the initial MUA–EDC/NHS modification produces a thin, relatively smooth organic coating, while introduction of GA2 leads to formation of thicker, uneven microstructures and enhanced surface roughness due to further cross-linking and molecular aggregation on the gold sensor surface.

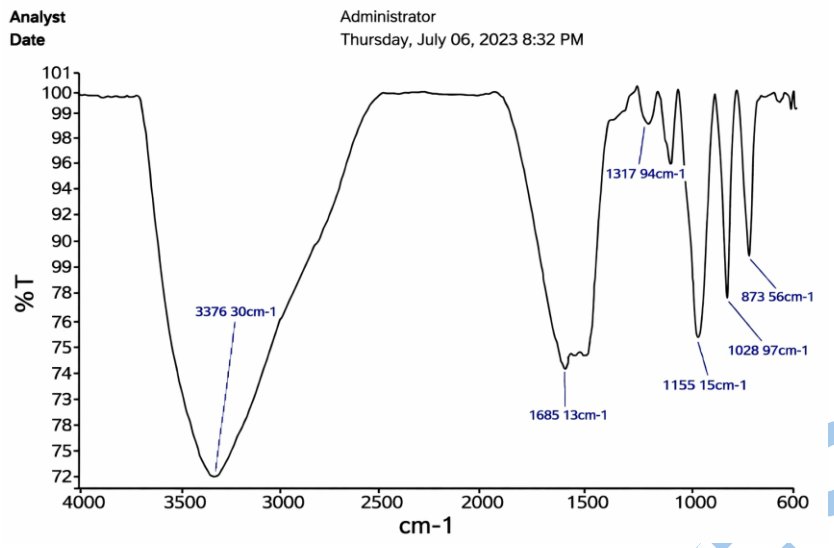

(A)

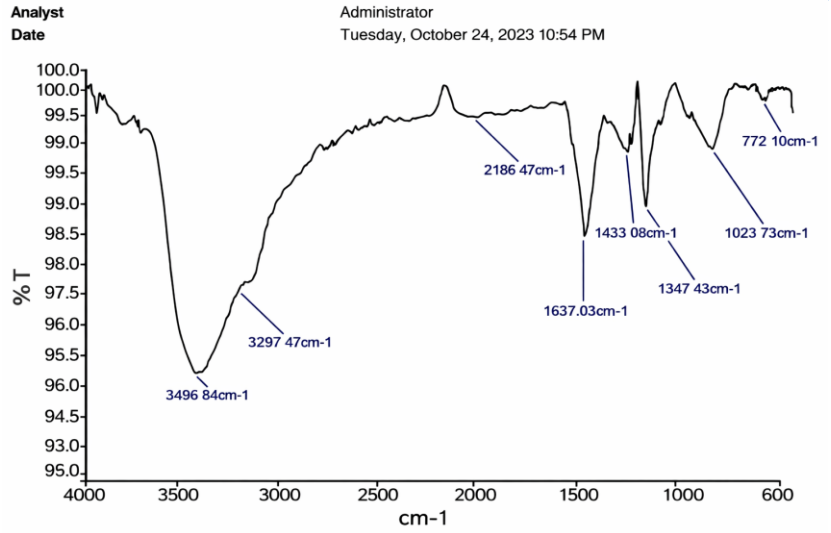

(B)

Figure 4. ATR-FTIR spectrum of (A) the raw sensor and (B) the sensor treated with ozone and UV.

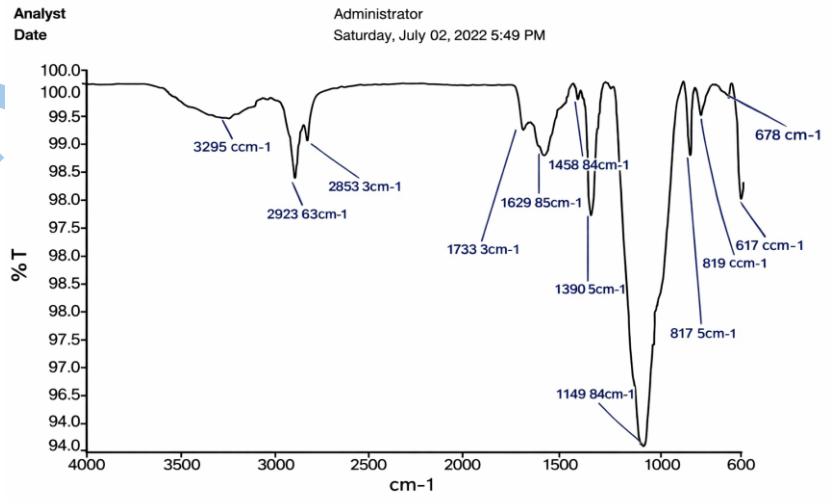

Figure 5. ATR-FTIR spectrum of the chemically treated sensor after immobilization of GA2.

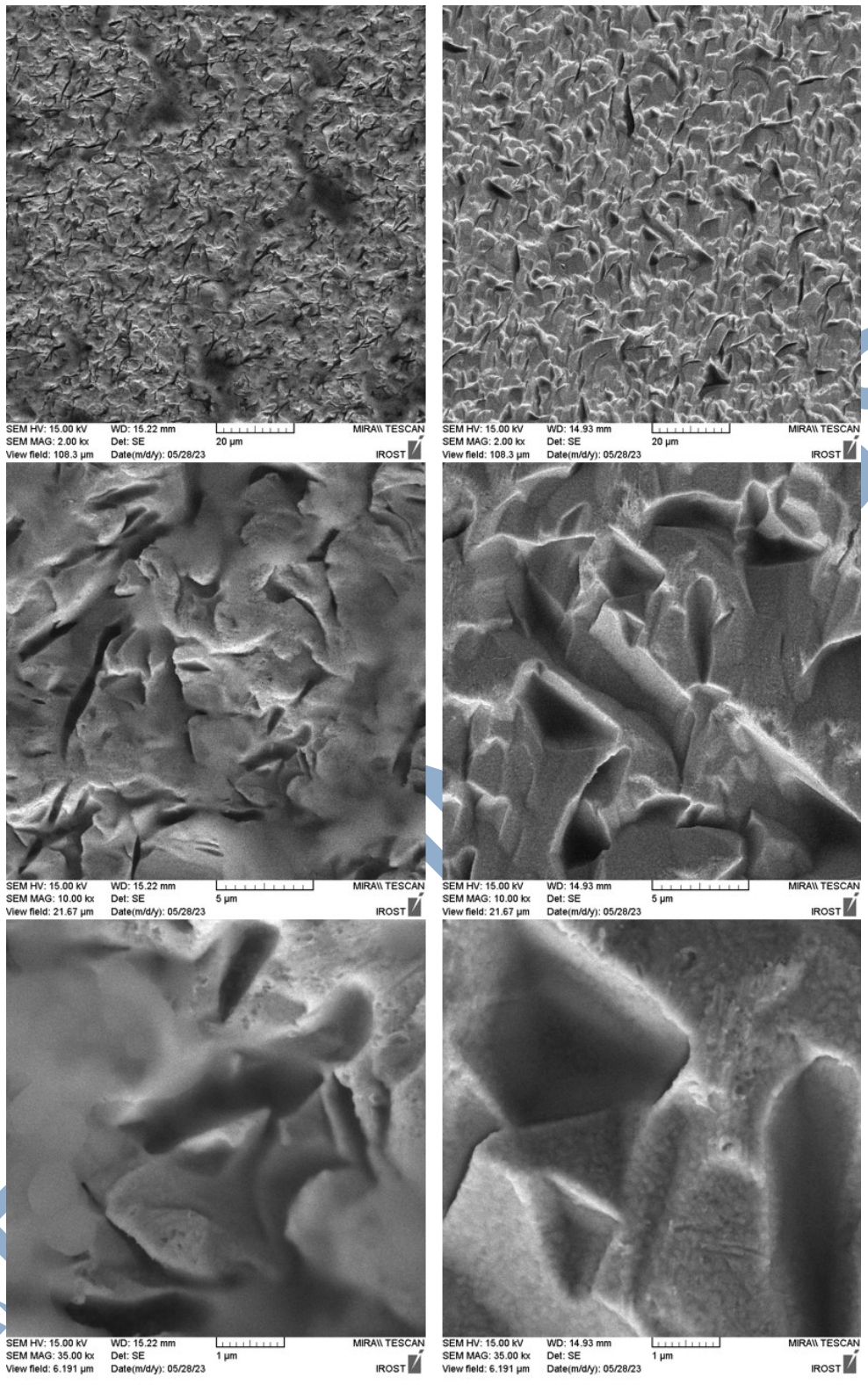

Figure 6. FESEM images of the sensor treated by MUA-EDC/NHS (left) and the treated sensor after immobilization of GA2 (right).

The efficiency of particle capture was then compared between GA2-coated and uncoated sensors. We compared the colony counts between coated and uncoated sensors under identical experimental conditions. Two identical cascade impactor samplers were used.

The samplers comprise four separation stages (A–D) that fractionate particles by aerodynamic diameter based on stage geometry and particle dynamics; therefore, given the typical dimensions of *S. aureus* cells, these bacteria were expected to deposit predominantly on stages C and D. For this reason, only these stages were analyzed in the experimental test. In Sampler 1, none of the sensors were coated; in Sampler 2, the sensor at Stage C was coated with GA2.

In one experiment, the test duration (including nebulization of the bacterial suspension and operation of the suction pump at approximately 4 L/min) was 3 minutes.

The results showed that the GA2-coated sensor at Stage C captured approximately 8.6 times more *S. aureus* cells than the uncoated control, confirming the enhancement predicted by the *in-silico* analysis. Table 3 presents the measured CFU values for coated and uncoated stages. Two other experiments were conducted to evaluate the repeatability of the results. In all experiments, *S. aureus* capture performance in stage C of the two cascade impactors was examined. One cascade impactor was considered as the reference device with an uncoated sensor, and the coated sensor was inserted in another cascade impactor as the control device.

Figure 7 shows the results of the ratio of coated-to-uncoated bacteria in these experiments. Also, we examined the device with *E. coli* as a control microorganism in one experiment. Figure 8 shows the ratio of the colony count in the test sampler (coated sensor at stages C and D) and the reference sampler (without coating). The results reveal the specificity of the device for *S. aureus* compared to *E. coli*.

The experimental in-vitro results reported here corroborate the in-silico predictions: the GA2 bio-coating on sensors within a cascade impactor considerably enhanced capture efficiency for *S. aureus* under the tested conditions.

Nonetheless, environmental conditions can influence final performance; for example, high humidity in the sampled air can reduce the effectiveness of the bio-coating. These in-vitro findings strongly align with the in-silico predictions, where GA2 demonstrated the highest binding affinity and the most stable interaction pattern with the ClfB receptor of S. aureus. The experimental results in bacterial capture on GA2-coated sensors confirm the enhanced receptor–ligand interaction suggested by docking and MD simulations, highlighting the strong agreement between computational modeling and practical performance.

In the final step of evaluating the sensor's coating quality, a surface analysis was conducted to compare a sensor with a new coating to one washed with distilled water and alcohol. The results are shown in Figure 9. Comparing these ATR-FTIR spectra indicates that washing and repeated use of the crystals do not significantly remove the active groups. Several factors have experimentally influenced the final adhesion results and, consequently, the sensor response:

- The type and characteristics of the coating, including hydrophilicity/hydrophobicity, elasticity, surface roughness, etc.
- Inlet air humidity
- Inlet air flow
- Competition between different particles and bacteria

By appropriately selecting these conditions, an optimal setting for better bacterial adhesion can be achieved, some of which are reflected in this report, and further investigations will be done in future research. The bio-receptor is an expensive but suitable method for bacterial capture. Naturally, choosing a more suitable coating method for GA2 will lead to better process results.

Table 3. Measured colony counts of *S. aureus* on Sampler stages C and D (CFU/ml).

	Stage C	**Stage D**
Sampler 1	No coating 8406	No coating 9354
Sampler 2	GA2 72000	No coating 6360
Fold-change in capture efficiency	= 8.6	

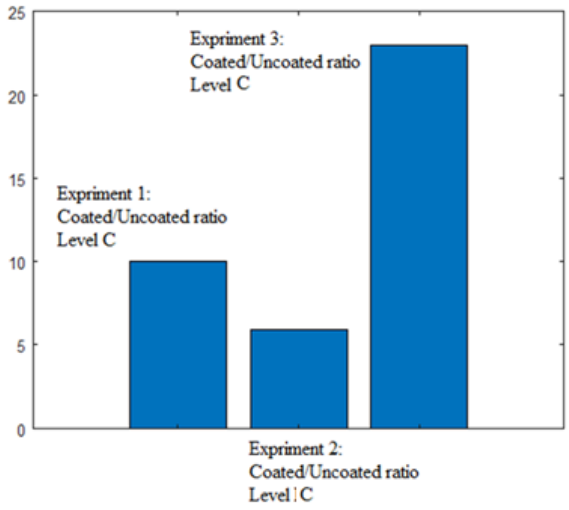

Figure 7. The results of three experiments (Refer to the text)

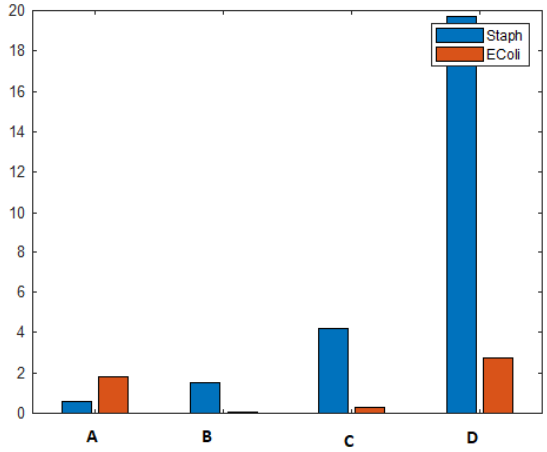

Figure 8. The normalized $\frac{test \text{ captured bacteria}}{reference \text{ captured bacteria}}$ for *E. coli* (Red bars) and *S. aureus* (Blue bars). (A, B, C and D are stages of the cascade impactor)

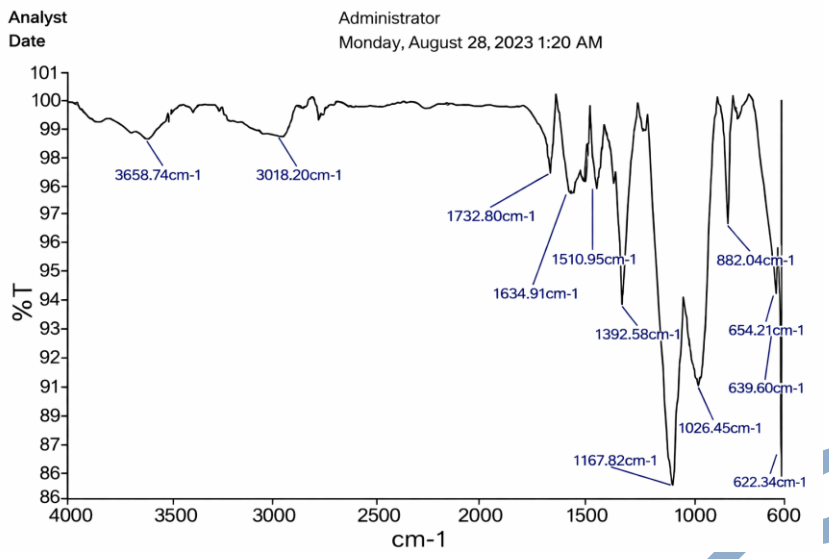

(A)

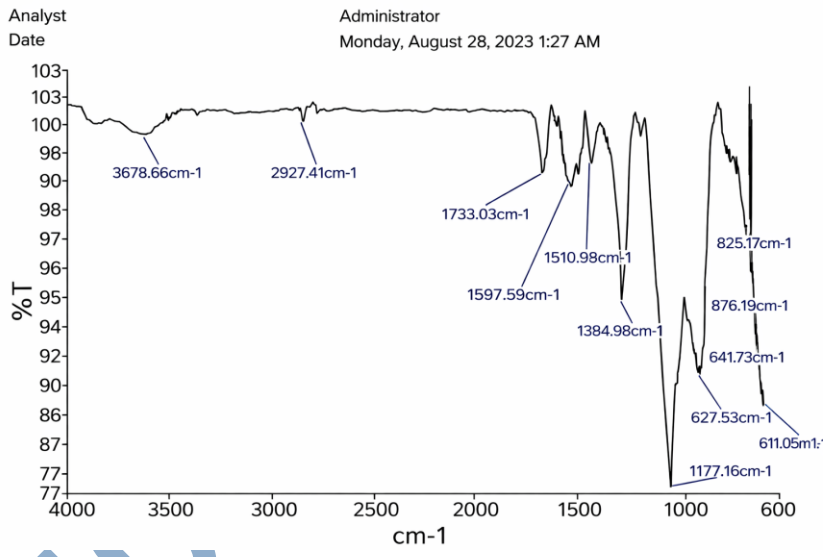

(B)

Figure 9. ATR-FTIR spectrum of (A) the freshly prepared coated sensor and (B) the disinfected coated sensor.

4. Conclusion

It should be noted that the current research highlights the promise of GA2 as a targeting ligand of the ClfB receptor in *S. aureus*. The experimental and simulation results can be used to develop specific therapeutics and diagnostics against this significant pathogen. Further research should involve longer molecular dynamics simulations under different environmental conditions in the in-vitro findings. Evaluating additional glycan analogs targeting ClfB may also contribute to further optimization of the specificity and effectiveness of the biosensor.

Conflict of interest

The authors declare no conflict of interest.

Acknowledgment

This research was supported by Nano PartaSen technologies Company. The authors would also like to thank Dr. Poopak Pir, Dr. Hamid Movahedian Attar, and Dr. Yaser Mohammadian Roshan for their technical and managerial advices. Also, the collaboration of Dr. Mohammad Haji-Abolhasani (IROST) for the coating of the sensor was appreciated.

Ethical approval

This article does not contain any studies with human participants or animals performed by any of the authors.

Funding

Nano PartaSen Technologies Company financially supported the research.

Authors' Contributions

VRN: Conceptualization, Investigation, Experiment Methodology, Validation, Writing – original draft, Writing – review & editing, **EFK:** Docking simulation, Investigation, Formal Analysis, Writing – original draft, Writing – review & editing, **ZM:** Conceptualization, Formal Analysis, Investigation, Experiment Methodology, Validation, Writing – original draft, Writing – review & editing, **YB:** Methodology, Validation, Writing – review & editing, **AB:** Methodology, Validation, Writing – review & editing. All authors have read and approved the final version of the manuscript.

Use of AI Tools

To enhance linguistic clarity and fluency, the authors utilized ChatGPT (OpenAI) during the editing process. The tool was used strictly for grammar improvement and language refinement. All scientific content, interpretation, and final approval were provided by the authors without automated generation of research findings.

References

Berry, K., Verhoef, M., Leonard, A., & Cox, G. (2022). Staphylococcus aureus adhesion to the host. *Ann. N. Y. Acad. Sci.*, *1515*(1), 75–96. https://doi.org/10.1111/nyas.14807

Brooks, B. R., BROOKS III, C. L., MACKERELL,A. D., NILSSON, L., PETRELLA, R. J., ROUX, B., WON, Y., ARCHONTIS, G., BARTELS, C., BORESCH, S., CAFLISCH, A., CAVES, L., CUI, Q., DINNER, A. R., FEIG, M., FISCHER, S., GAO, J., HODOSCEK, M., IM, W., KUCZERA, K., LAZARIDIS, T., MA, J., OVCHINNIKOV, V., PACI, E., PASTOR, R. W., POST, C. B., PU, J. Z., SCHAEFER, M., TIDOR, B., VENABLE, R. M., WOODCOCK, H. L., WU, X., YANG, W., YORK, D. M., KARPLUS6, M. (2009). CHARMM: The biomolecular simulation program. *J. Comput. Chem.*, *30*(10), 1545–1614. https://doi.org/10.1002/jcc.21287

Crosby, H. A., Kwiecinski, J., & Horswill, A. (2017). Staphylococcus Aureus aggregation and coagulation mechanisms, and their function in host-pathogen interactions. *Adv. Appl. Microbiol.*, *96*, 1–40. https://doi.org/10.1016/bs.aambs.2016.07.018

Croxen, M., Law, R., Scholz, R., Keeney, K., Wlodarska, M., Finlay, B. (2013). Recent advances in understanding enteric pathogenic Escherichia Coli. *Clin. Microbiol. Rev.*, *26*(4), 822–80. https://doi.org/10.1128/CMR.00022-13

Eswar, N., Webb, B., Marti-Renom, M., Madhusudhan, M. S., Eramian, D., Shen, M., Pieper, U., Sali, A. (2006). Comparative protein structure modeling using modeller. *Curr. Protoc. Bioinform.*, *15*(1), 5.6.1-5.6.30. https://doi.org/10.1002/0471250953.bi0506s15

Forli, S., Huey, R., Pique, M., Sanner, M., Goodsell, D., Olson, A. (2016). Computational protein-ligand docking and virtual drug screening. *Nat. Protoc.*, *11*(5), 905–19. https://doi.org/10.1038/nprot.2016.051

Foster, T., Geoghegan, J., Ganesh, V., & Höök, M. (2014). Adhesion, invasion and evasion: the many functions of the surface proteins of Staphylococcus Aureus. *Nat. Rev. Microbiol.*, *12*(1), 49–62. https://doi.org/10.1038/nrmicro3161

Ganesh, V., Rivera, J., Smeds, E., Ko, Y., Bowden, M., Wann, E., Gurusiddappa, S., Fitzgerald, J., Hook, M. (2008). A structural model of the Staphylococcus Aureus ClfA – fibrinogen interaction opens new avenues for the design of anti-Staphylococcal therapeutics. *PLoS Pathog.*, *4*(11), e1000226. https://doi.org/10.1371/journal.ppat.1000226

Ganesh, V., Barbu, E., Deivanayagam, C., Le, B., Anderson, A., Matsuka, Y., Lin, S., Foster, T., Narayana, S., Hook, M. (2011). Structural and biochemical characterization of Staphylococcus Aureus Clumping Factor B/ligand interactions. *J. Biol. Chem.*, *286*(29), 25963–72. https://doi.org/10.1074/jbc.M110.217414

Ghali, H., Chibli, H., Nadeau, J., Bianucci, P., Peter, Y. (2016). Real-time detection of Staphylococcus Aureus using whispering gallery mode optical microdisks. Biosens*ors*, *6*(2), 20. https://doi.org/10.3390/bios6020020

Leach, A., Shoichet, B., & Peishoff, C. (2006). Prediction of protein-ligand interactions. Docking and scoring: successes and gaps. *J. Med. Chem.*, *49*(20), 5851–55. https://doi.org/10.1021/jm060999m

Li, Y., Poole, S., Rasulova, F., McVeigh, A., Savarino, S., Xia, D. (2007). A receptor-binding site as revealed by the crystal structure of CfaE, the colonization Factor Antigen I Fimbrial adhesin of enterotoxigenic Escherichia Coli. *J. Biol. Chem.*, *282*(33), 23970–80. https://doi.org/10.1074/jbc.M700921200

Martínez-Alonso, M., González-Montalbán, N., García-Fruitós, E., & Villaverde, A. (2008). The functional quality of soluble recombinant polypeptides produced in Escherichia Coli is defined by a wide conformational spectrum. *Appl. Environ. Microbiol.*, *74*(23), 7431–33. https://doi.org/10.1128/AEM.01446-08

Nataro, J., & Kaper, J. (1998). Diarrheagenic Escherichia Coli. *Clin. Microbiol. Rev.*, *11*(1), 142–201. https://doi.org/10.1128/cmr.11.1.14

Otto, M. (2013). Staphylococcal infections: mechanisms of biofilm maturation and detachment as critical determinants of pathogenicity. *Annu. Rev. Med.*, *64*, 175–88. https://doi.org/10.1146/annurev-med-042711-140023

Reddinger, R., Luke-Marshall, N., Hakansson, A., & Campagnari, A. (2016). Host physiologic changes induced by influenza a virus lead to Staphylococcus Aureus biofilm dispersion and transition from asymptomatic colonization to invasive disease. *mBio*, *7*(4), e01235-16. https://doi.org/10.1128/mBio.01235-16

Schwermann, N., & Volker, W. (2023). Functional diversity of Staphylococcal Surface proteins at the host-microbe interface. *Front. Microbiol.*, *14*, 1196957. https://doi.org/10.3389/fmicb.2023.1196957

Tong, S., Davis, J., Eichenberger, E., Holland, T., Fowler, V., Jr. (2015). Staphylococcus Aureus infections: epidemiology, pathophysiology, clinical manifestations, and management. *Clin. Microbiol. Rev.*, *28*(3), 603–61. https://doi.org/10.1128/CMR.00134-14

Varki, A. (2007). Glycan-based interactions involving vertebrate Sialic-Acid-Recognizing proteins. *Nature*, *446*(7139), 1023–29. https://doi.org/10.1038/nature05816

Wertheim, H., Walsh, E., Choudhurry, R., Melles, D., Boelens, H., Miajlovic, H., Verbrugh, H., Foster, T., Belkum, A. (2008). Key role for Clumping Factor B in Staphylococcus Aureus nasal colonization of humans. *PLoS Med.*, *5*(1), e104. https://doi.org/10.1371/journal.pmed.0050017

Zelada-Guillén, G., Sebastián-Avila1, J., Blondeau, P., Riu, J., Rius, F. (2012). Label-Free detection of Staphylococcus Aureus in skin using real-time potentiometric biosensors based on carbon nanotubes and aptamers. *Biosens. Bioelectron.*, *31*(1), 226–32. https://doi.org/10.1016/j.bios.2011.10.021

Zhang, Y., Tan, P., Zhao, Y., & Ma, X. (2022). Enterotoxigenic Escherichia Coli: intestinal pathogenesis mechanisms and colonization resistance by gut microbiota. *Gut Microbes*, *14*(1), 2055943. https://doi.org/10.1080/19490976.2022.2055943

How to cite this paper:

Nafisi, VR., Fahimi Kashani, E., Mousavian, Z., Bide, Y., & Balaei, A. (2025). Theoretical and Experimental Study of a Glycan-Coated Biosensor for *Staphylococcus aureus* Detection. *Microbiology, Metabolites and Biotechnology, 7*(2), 109-114.
DOI: 10.22104/mmb.2025.7874.1184